

Propagation of a deuteron in nuclear matter and the spin dependence of the deuteron optical potential

A. A. Ioannides and R. C. Johnson

Department of Physics, University of Surrey, Guildford, Surrey, GU2 5XH England

(Received 8 August 1977)

The propagation of a deuteron through nuclear matter is examined in terms of a simple nonlocal but separable potential for the n - p interaction. It is found that the binding energy of the deuteron in nuclear matter depends strongly on the relative orientation of the deuteron spin and center-of-mass momentum, when both the Pauli exclusion principle and the tensor force component in the neutron-proton interaction are included in the calculation. A thorough discussion of the physical mechanism involved is presented. It is shown that this effect is associated with the presence of a new type of spin dependent interaction of the T_p type, in the deuteron-nucleus optical potential. The nuclear matter calculations are applied to the realistic case of a deuteron scattered by a heavy nucleus through a simple model which is valid for deuteron incident energies in excess of 100 MeV. The T_p force thus produced is found to have a non-negligible strength over a wide range of high incident deuteron energies and to be very sensitive to high momentum components of the nucleon-nucleon interaction. The mechanism examined here is also expected to generate a T_p force and a modified T_R force at low energies.

[NUCLEAR REACTIONS d in nuclear matter, Pauli exclusion principle, D -state] probability. d optical potential, tensor force, $E_d < 1$ BeV, polarized d .

I. INTRODUCTION

This paper is concerned with the effects of antisymmetrization on the scattering of a deuteron by a heavy target nucleus. As a simple model it is assumed that the target remains in its ground state and is adequately described throughout the scattering by a single determinant of occupied single-particle states. Models of this type have been studied by a number of authors¹⁻⁶ and are known to provide a framework within which interesting physical effects associated with antisymmetrization can be displayed and calculated. The relevant literature has been reviewed recently by Pong and Austern.⁵

Under these assumptions the deuteron-nucleus many-body Schrödinger equation reduces to an effective three-body equation for a function $\psi(p, n)$ of the coordinates of a neutron and proton only. The equation satisfied by this function is of the Bethe-Goldstone type and can be written

$$(E - t_p - t_n - U_p - Q V_{np})\psi(p, n) = 0, \quad (1)$$

where t_p and t_n are kinetic energy operators for the proton and neutron, U_p and U_n are Hartree-Fock potentials for the nucleon-nucleus interaction, and V_{np} is the neutron-proton interaction. The influence of the identity of the nucleons in the deuteron and the nucleons in the target is displayed in Eq. (1) through the operator Q which projects onto states of the two nucleon system which can be constructed out of single-particle states not occupied in the target ground state.

Approximate solutions of Eq. (1) and a discussion of implications for the deuteron optical potential can be found in Ref. 5 where a review of earlier calculations based on versions of Eq. (1) can also be found. Reference 5 also contains an estimate of target excitation effects neglected in Eq. (1).

This paper is primarily concerned with the additional physical effects that arise in the solution of Eq. (1) because of the large tensor force component of V_{np} . These effects have been ignored in earlier work in this field which has emphasized corrections to the central part of the deuteron optical potential. It will be shown here that the combined effects of the tensor force in V_{np} and the requirements of antisymmetry give rise to a significant spin-dependent force in the deuteron optical potential of the T_p type (in Satchler's⁷ classification).

In order to display this result in a simple context the case of a deuteron propagating in nuclear matter is considered in the next section. The implications of the nuclear matter results for deuteron scattering by a finite nucleus are discussed in Sec. III. A brief account of some of these results has been given in Ref. 8.

II. DEUTERON IN NUCLEAR MATTER

A. Bound state solutions of the Bethe-Goldstone equation

In this section the neutron and proton of Eq. (1) are assumed to be propagating in nuclear matter in its ground state and of uniform density char-

acterized by a Fermi momentum k_F . The projector Q is taken to be

$$Q = Q_p Q_n, \quad (2)$$

where

$$Q_p = \int_{k_p > k_F} d\vec{k}_p \sum_{\sigma_p} |\vec{k}_p, \sigma_p\rangle \langle \vec{k}_p, \sigma_p|, \quad (3)$$

where $|\vec{k}_p, \sigma_p\rangle$ is a plane wave proton state. A similar definition obtains for Q_n .

In nuclear matter the Hamiltonian in (1) commutes with the operator for the total momentum of the neutron and proton and Eq. (1) has solutions of the form

$$\psi = e^{i\vec{K}\cdot\vec{R}} \phi_{\vec{K},\epsilon}(\vec{r}), \quad (4)$$

where

$$\vec{R} = \frac{1}{2}(\vec{r}_p + \vec{r}_n), \quad \vec{r} = \vec{r}_p - \vec{r}_n, \quad (5)$$

and $\phi_{\vec{K},\epsilon}(\vec{r})$ satisfies

$$(\epsilon - t_r - Q\tilde{K}(k_F)V_{np})|\phi_{\vec{K},\epsilon}\rangle = 0, \quad (6)$$

with

$$E = \epsilon + \frac{\hbar^2 K^2}{4m} + U_p^{(0)} + U_n^{(0)}, \quad (7a)$$

$$t_r = -\frac{\hbar^2}{m} \nabla_r^2, \quad (7b)$$

and m is the nucleon mass. The operator $Q\tilde{K}(k_F)$ in Eq. (6) acts on the spins and relative coordinates of the neutron and proton only and is given by

$$Q\tilde{K}(k_F) = \sum_{\sigma_p, \sigma_n} \int d\vec{k} |\vec{k}, \sigma_p, \sigma_n\rangle \langle \vec{k}, \sigma_p, \sigma_n| \times \theta_{k_F}(\vec{K}, \vec{k}), \quad (8)$$

where

$$\begin{aligned} \theta_{k_F}(\vec{K}, \vec{k}) &= 0, \quad \text{if } |\frac{1}{2}\vec{K} + \vec{k}| \text{ or } |\frac{1}{2}\vec{K} - \vec{k}| \\ &\quad \text{is less than } k_F, \\ &= 1, \quad \text{if } |\frac{1}{2}\vec{K} + \vec{k}| \text{ and } |\frac{1}{2}\vec{K} - \vec{k}| \\ &\quad \text{are greater than } k_F \end{aligned} \quad (9)$$

and

$$\langle \vec{r} | \vec{k} \rangle = \frac{e^{i\vec{k}\cdot\vec{r}}}{(2\pi)^{3/2}}. \quad (10)$$

In writing down Eqs. (6) and (7) the nonlocality of the Hartree-Fock potentials U_n and U_p has been ignored in order to simplify the formulas, and $U_n^{(0)}$ and $U_p^{(0)}$ are taken to have the constant values $U_n^{(0)}$ and $U_p^{(0)}$. A simple correction for nonlocality is included later along the lines studied in Refs. 9 and 10.

Bound state solutions of (6) with $\epsilon < 0$ also satisfy

$$|\phi_{\vec{K},\epsilon}\rangle = \frac{1}{\epsilon - t_r} Q\tilde{K}(k_F)V_{np}|\phi_{\vec{K},\epsilon}\rangle. \quad (11)$$

Solutions of this equation exist in simple analytic form if V_{np} is a separable interaction. They have been studied in detail by Gambhir and Griffin⁴ in the case that V_{np} is the rank-1 S-wave potential of Yamaguchi.¹¹ It was shown in Ref. 4 that bound state solutions exist for sufficiently high E , or low enough k_F .

The treatment is readily extended to the case when V_{np} contains a tensor force of the type given by Yamaguchi and Yamaguchi¹² which has the form

$$V_{np} = -\frac{\hbar^2 \lambda}{m} \sum_{M=-1}^{+1} |f_M\rangle \langle f_M|, \quad (12)$$

where

$$\langle \vec{k}, \sigma_p, \sigma_n | f_M \rangle = \left[C(k) + \frac{1}{\sqrt{8}} T(k) S_{12}(\vec{k}) \right] \chi_{1M}(\sigma_p, \sigma_n), \quad (13)$$

In Eq. (13) χ_{1M} is a triplet spin wave function and S_{12} is the usual tensor force operator

$$S_{12}(\vec{k}) = \frac{3[\vec{\sigma}(p) \cdot \vec{k}][\vec{\sigma}(n) \cdot \vec{k}]}{k^2} - \vec{\sigma}(p) \cdot \vec{\sigma}(n). \quad (14)$$

The particular functional forms assumed in Ref. 12 for $C(k)$ and $T(k)$ were

$$C(k) = \frac{1}{\beta^2 + k^2}, \quad (15a)$$

$$T(k) = \frac{-tk^2}{(\gamma^2 + k^2)^2}, \quad (15b)$$

where the force parameters λ , t , γ , and β were chosen to fit properties of the deuteron and low energy n - p scattering. According to Ref. 12 this procedure gives

$$\lambda = 0.2540 \text{ fm}^{-3}, t = 1.663, \quad (16a)$$

$$\beta = 1.335 \text{ fm}^{-1}, \gamma = 1.537 \text{ fm}^{-1} \quad (16b)$$

if the deuteron D -state probability is assumed to be 4%. Alternative sets of values of these parameters will be discussed below.

Because of the way the direction \vec{K} is picked out by the operator $Q\tilde{K}(k_F)$ in Eq. (11) the angular momentum about the center of mass of the deuteron \vec{J} does not commute with $Q\tilde{K}(k_F)V_{np}$ even though it commutes with V_{np} , and hence eigenstates $|\phi_{\vec{K},\epsilon}\rangle$ do not have definite \vec{J} . However, $\vec{J} \cdot \vec{K}$ does commute with $Q\tilde{K}(k_F)V_{np}$, and hence solutions of Eq. (11) have the form

$$|\phi(\vec{K}, \epsilon_M, M)\rangle = N_M \frac{1}{\epsilon_M - t_r} Q\tilde{K}(k_F)|f_M\rangle, \quad (17)$$

provided ϵ_M satisfies

$$1 + \frac{\hbar^2 \lambda}{m} \langle f_M | \frac{1}{\epsilon_M - t_r} Q_{\vec{K}}(k_F) | f_M \rangle = 0. \quad (18)$$

In these expressions N_M is a normalization constant, and the quantum number M is the eigenvalue of $\vec{J} \cdot \vec{K}/K$, i.e., choosing the z axis to be along the direction of \vec{K}

$$J_z | \phi(\vec{K}, \epsilon_M, M) \rangle = M | \phi(\vec{K}, \epsilon_M, M) \rangle. \quad (19)$$

If V_{np} is invariant under time reversal it is not difficult to show that

$$\epsilon_M = \epsilon_{-M}. \quad (20)$$

Equations (17)–(20) mean that a deuteron with center-of-mass momentum \vec{K} which is triply degenerate in free space ($M = \pm 1, 0$), splits in nuclear matter into two states of different energy: a nondegenerate state with $M = 0$, energy ϵ_0 , and a doubly degenerate state with $M = \pm 1$, and energy ϵ_1 , where M is the component of the total angular momentum along \vec{K} .

The eigenvalues ϵ_M are the values of ϵ which satisfy Eq. (18). This can be rewritten

$$1 + \frac{\hbar^2 \lambda}{m} V_M(\epsilon) = 0, \quad (21a)$$

where

$$V_M(\epsilon) = \langle f_M | \frac{1}{\epsilon - t_r} Q_{\vec{K}}(k_F) | f_M \rangle. \quad (21b)$$

The difference $\epsilon_1 - \epsilon_0$ is nonzero only if the nuclear matter density is nonzero and the tensor force component in V_{np} is nonzero. If $k_F = 0$, $Q_{\vec{K}}$ is independent of the direction of \vec{K} , and V_M becomes independent of M because it is the matrix element of a tensor of rank zero in spin and relative coordinate space. In the absence of tensor forces $V_M(\epsilon)$ is independent of M even if $k_F \neq 0$ because then $|f_M\rangle$ is an eigenfunction of the intrinsic spin operators \vec{S}^2 and S_z and the operators $Q_{\vec{K}}$ and $(\epsilon - t_r)^{-1}$ are tensors of rank zero in spin space.

The general nature of some of these results can be seen by noting that if $|\phi(\vec{K}, \epsilon_M, M)\rangle$ is a normalized solution of Eq. (11), and ϵ_M satisfies Eq. (18), then also

$$\begin{aligned} \epsilon_M &= \langle \phi(\vec{K}, \epsilon_M, M) | [t_r + Q_{\vec{K}}(k_F) V_{np}] | \phi(\vec{K}, \epsilon_M, M) \rangle \\ &= \langle \phi(\vec{K}, \epsilon_M, M) | Q_{\vec{K}}(k_F) (t_r + V_{np}) Q_{\vec{K}}(k_F) | \phi(\vec{K}, \epsilon_M, M) \rangle \\ &= \langle \phi(\vec{K}, \epsilon_M, M) | H_{np} | \phi(\vec{K}, \epsilon_M, M) \rangle, \end{aligned} \quad (22)$$

where

$$H_{np} = t_r + V_{np} \quad (23)$$

is the free-space Hamiltonian for the n - p system. The state $|\phi(\vec{K}, \epsilon_M, M)\rangle$ can be regarded as a trial wave function for an eigenstate of H_{np} with $J_z = M$, and therefore

$$\epsilon_M \geq \epsilon_M^0, \quad (24)$$

where ϵ_M^0 is the lowest eigenvalue of H_{np} with $J_z = M$.

The result (24) means, for example, that a deuteron is always less bound in nuclear matter than in free space. In addition, (24) can be used to show that the connection between the presence of spin-dependent forces in the spin-triplet V_{np} and the existence of two bound states with different binding energies for the n - p system in nuclear matter is a very general one and is not a peculiarity of the Yamaguchi potential. Thus, consider a spin-independent spin-triplet V_{np} adjusted to give the correct spectrum of H_{np} in free space. The ground state will be characterized by $L = L_z = 0$, and all other states will be unbound. The spin wave functions can be ignored and Eqs. (22) and (23) can be used with M reinterpreted as L_z . In nuclear matter \vec{L}^2 is not a good quantum number even in the absence of tensor forces; nevertheless the inequality (24) shows that there can be no bound states with $L_z \neq 0$ because all eigenstates of H_{np} with $L_z \neq 0$ are unbound in free space.

Of course, whether or not any states are bound for an interesting range of values of K^2 and k_F depends on the values of the parameters determining V_{np} . This question will be taken up in Sec. II D.

B. Calculation of binding energy

In order to evaluate the quantity $V_M(\epsilon)$ of Eq. (18) it is convenient to use the Legendre expansions of the projection operator $Q_{\vec{K}}$. Using properties of the Legendre polynomials $P_l(x)$ it is readily shown that the quantity $\theta_{k_F}(\vec{K}, \hat{k})$ defined in Eqs. (8)–(10) has the expansion

$$\theta_{k_F}(\vec{K}, \hat{k}) = \frac{1}{2} \sum_l \theta_l(K, k, k_F) (2l+1) P_l(\hat{K} \cdot \hat{k}), \quad (25)$$

where \hat{K} denotes the direction of \vec{K} , and where

$$\theta_l(K, k, k_F) = 0, \quad l \text{ odd}, \quad (26a)$$

$$\begin{aligned} \theta_0(K, k, k_F) &= 2b\theta(k-a)\theta(k_F + \frac{1}{2}K - k) \\ &\quad + 2[\theta(\frac{1}{2}K - k_F - k) + \theta(k - \frac{1}{2}K - k_F)], \end{aligned} \quad (26b)$$

$$\begin{aligned} \theta_l(K, k, k_F) &= \frac{2(b^2 - 1)P'_l(b)}{l(l+1)} \theta(k-a)\theta(k_F + \frac{1}{2}K - k), \\ &\quad l > 0, \text{ even}, \end{aligned} \quad (26c)$$

and a and b are defined by

$$a(K, k, k_F) = \begin{cases} \frac{1}{2}K - k_F, & \text{if } k_F < \frac{1}{2}K, \\ (k_F^2 - \frac{1}{4}K^2)^{1/2}, & \text{if } k_F > \frac{1}{2}K, \end{cases} \quad (27a)$$

$$b(K, k, k_F) = \frac{k^2 + \frac{1}{4}K^2 - k_F^2}{Kk}. \quad (27b)$$

The form factor given in Eq. (13) can also be written

$$\langle \hat{k}, \sigma_p, \sigma_n | f_M \rangle = (4\pi)^{1/2} \sum_{L=0,2} v_L(k) Y_{(L1)1}^M(\hat{k}, \sigma_p, \sigma_n), \quad (28)$$

where

$$Y_{(LS)\lambda}^M(\hat{k}, \sigma_p, \sigma_n) = \sum_{\lambda_0} (L\lambda, S\sigma | JM) Y_{L\lambda}(\hat{k}) \chi_{S\sigma}(\sigma_p, \sigma_n), \quad (29)$$

$$v_0(k) = C(k), \quad (30a)$$

$$v_2(k) = T(k). \quad (30b)$$

Standard formulas¹³ can now be used to show that the quantity $V_M(\epsilon)$ defined in Eq. (21) can be expressed as

$$\begin{aligned} \frac{\hbar^2}{m} V_M(\epsilon) = & - \sum_L (1M, l0 | 1M) \\ & \times \sum_{L', L''} \sqrt{3} \hat{L}^2 \hat{L}'^2 (L0, l0 | L'0) W(L' L 11; l1) \\ & \times 2\pi \int_0^\infty dk k^2 v_{L'}(k) \frac{1}{\Delta^2 + k^2} \\ & \times v_L(k) \theta_l(K, k, k_F), \end{aligned} \quad (31)$$

where Δ^2 is defined by $\epsilon = -\hbar^2 \Delta^2 / m$, and $\hat{L} = (2L+1)^{1/2}$.

Tables¹⁴ of the angular momentum coupling coefficients can be used to reduce Eq. (31) to

$$\frac{\hbar^2}{m} V_{\pm 1}(\epsilon) = -I_0(\epsilon) + I_2(\epsilon), \quad (32a)$$

$$\frac{\hbar^2}{m} V_0(\epsilon) = -I_0(\epsilon) - 2I_2(\epsilon), \quad (32b)$$

where

$$I_0(\epsilon) = 2\pi \int_0^\infty dk k^2 \theta_0(K, k, k_F) \frac{C^2(k) + T^2(k)}{\Delta^2 + k^2}, \quad (33a)$$

$$I_2(\epsilon) = 2\pi \int_0^\infty dk k^2 \theta_2(K, k, k_F) \frac{T(k) [\frac{1}{2}T(k) - \sqrt{2}C(k)]}{\Delta^2 + k^2}. \quad (33b)$$

The eigenvalue condition given in Eq. (21a) becomes

$$\lambda = \frac{1}{I_0(\epsilon_1) - I_2(\epsilon_1)}, \quad M = \pm 1, \quad (34a)$$

$$\lambda = \frac{1}{I_0(\epsilon_0) + 2I_2(\epsilon_0)}, \quad M = 0, \quad (34b)$$

where

$$\epsilon_M = -\frac{\hbar^2}{m} \Delta^2(M, K, k_F) \quad (35a)$$

and

$$B_M = -\epsilon_M \quad (35b)$$

is the binding energy of a deuteron with the quantum numbers displayed as arguments of Δ in Eq. (35).

Note that in free space, where $\theta_2 = 0$ for all k , or in the absence of a tensor force, when $T(k) = 0$ for all k , the integral $I_2(\epsilon)$ vanishes, the two eigenvalue conditions (34) become identical, and the deuteron binding energy becomes independent of the relative orientation of its linear and angular momenta, as expected.

For the functional forms given in Eq. (15) the integrals in Eq. (33) can be evaluated analytically for a given set of values of the force parameters t, γ, β , center-of-mass momentum K , Fermi momentum k_F , and binding energy parameter Δ . The approach used to solve Eqs. (34a) and (34b) was to vary the value of Δ in each case such that the right-hand sides yielded the correct value of the free-space n - p force strength λ . The results were checked by evaluating the integrals I_0 and I_2 both numerically and analytically.¹⁵

C. Parameters of V_{np}

As a measure of the sensitivity of the results discussed in the next section to the model assumed for the neutron-proton interaction in free space a number of calculations were performed with different values of the range parameters β and γ , and the strength parameters λ and t . It was found possible to adjust the predicted free-space deuteron D -state probability by large factors while keeping the free-space deuteron binding energy, quadrupole moment Q , and triplet scattering length fixed at their experimental values. At the same time the predicted triplet effective range changed by very small amounts so that the sets of parameters obtained in this way all fitted the very low energy properties of the triplet n - p system well. Sets of parameters corresponding to different D -state probabilities therefore correspond to different models of the high energy short distance behavior of the neutron-proton interaction. Further details can be found in the Appendix where a table of sets of parameters can be found.

D. Numerical results for the binding energy in nuclear matter

The term "para state" will be used to refer to a state with $M = \pm 1$. In these cases the deuteron's angular momentum has a nonvanishing projection

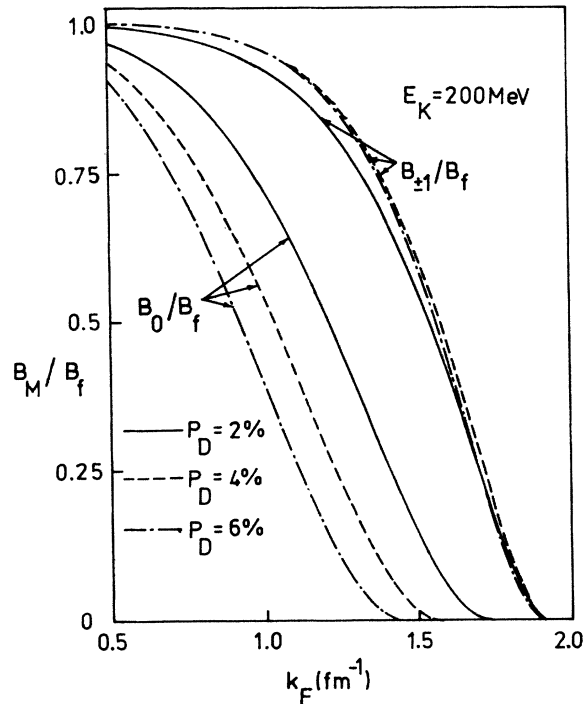


FIG. 1. Binding energy for the para state and ortho state in nuclear matter for deuteron energy 200 MeV and the indicated D -state probabilities.

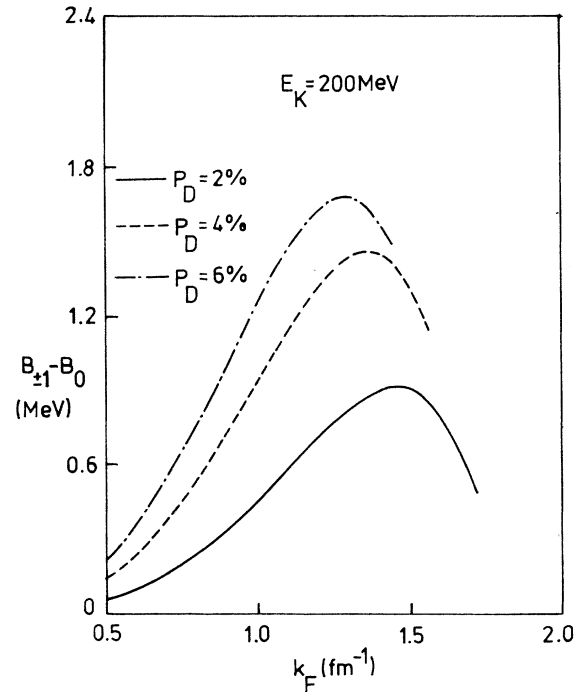


FIG. 2. Binding energy difference between the para state and ortho state in nuclear matter for deuteron energy 200 MeV and indicated D -state probabilities.

along its center-of-mass momentum \vec{K} . A state having a vanishing angular momentum projection along \vec{K} , i.e., $M=0$, will be referred to an an "ortho state".

Figure 1 shows the variation with k_F of the ratio of the deuteron binding energy to B_f , the deuteron binding energy in free space. The center-of-mass momentum K corresponds to an energy

$$E_K = \hbar^2 K^2 / 4m \quad (36)$$

of 200 MeV. This energy is appropriate for a deuteron at the center of a heavy nucleus whose kinetic energy outside the nucleus is roughly 120 MeV.

The curves corresponding to different free-space D -state probabilities P_D in Fig. 1 refer to the parameter sets for the n - p interaction discussed in Sec. II C.

In Fig. 2 the difference between the binding energies of the ortho and para states is displayed for the same cases as in Fig. 1. The dependence of the binding energy ratio and differences on E_K for a Fermi momentum corresponding to the center of a heavy nucleus is shown in Figs. 3 and 4.

Note that the curves break off in Fig. 2 at high k_F and in Fig. 4 at low K because at these points

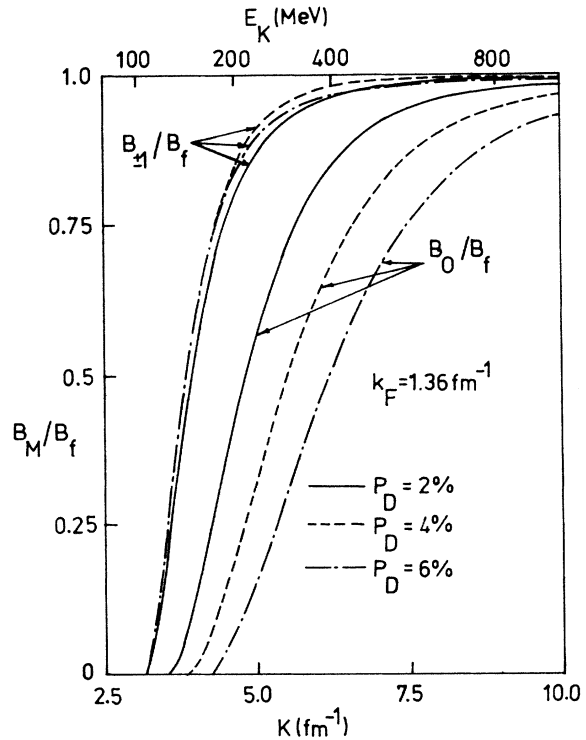


FIG. 3. Binding energy for the para state and ortho state in nuclear matter of Fermi momentum 1.36 fm^{-1} and the indicated D -state probabilities.

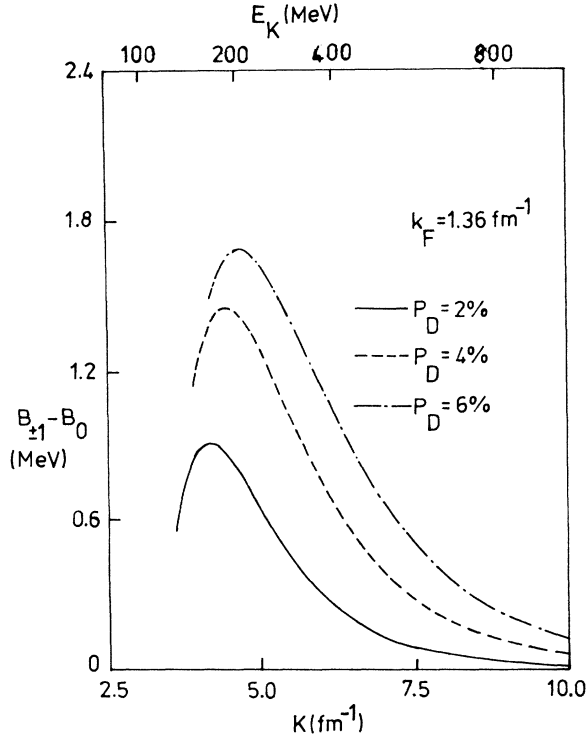


FIG. 4. Binding energy difference between the para and ortho state in nuclear matter of Fermi momentum 1.36 fm^{-1} and the indicated D -state probabilities.

the binding energy of the ortho state goes to zero. A method of extending the results beyond these points is discussed in Ref. 6. This approach will not be followed here because it will be shown in Sec. III B that the application of these results to finite nuclei is most valid at high energy. Some important features of these results are set out below.

(i) The binding energy of the deuteron in nuclear matter is always less than the binding energy in free space. The general reason for this is discussed in Sec. II A [see Eq. (24)]. Note that the figures show that the free space binding energy is achieved for $k_F \rightarrow 0$ as expected.

(ii) The binding energy of the para states is always greater than the binding energy of the ortho state, i.e., $B_{\pm 1} > B_0$. The ortho-state binding energy goes to zero with increasing density (Fig. 1) or decreasing K (Fig. 3) much more rapidly than the para-state binding energy.

(iii) The energy difference $(B_{\pm 1} - B_0)$ has a maximum as a function of E_K , for fixed k_F . There is no splitting for $K = 0$ because no direction is picked out to which M can refer in that limit; there is no splitting for $K \rightarrow \infty$ because B_M approaches B_1 for all M . Hence the energy difference must have at least one maximum as a function of E_K . A sim-

ilar discussion shows that the observed maximum as a function of k_F , for fixed E_K , is consistent with the expected behavior of the energy difference in the limit of large and small k_F .

(iv) When the parameters of V_{np} are varied such that the free-space deuteron binding energy, quadrupole moment, scattering length, and effective range are essentially constant, but the free-space D -state probability P_D is allowed to change by a substantial amount, large changes are induced in the binding energy of the ortho state B_0 . The relatively small changes in $B_{\pm 1}$ show a complicated dependence on P_D , but the binding energy of the ortho state decreases systematically with an increase of P_D . As a result $(B_{\pm 1} - B_0)$ increases with P_D (see Fig. 4).

The relevance of these results to the propagation of a deuteron through a finite nucleus will be discussed in Sec. III. The next several subsections are concerned with obtaining an understanding of the systematic effects described in paragraphs (i)–(iv) above, and to this end the angular momentum distribution of the wave function of a deuteron in nuclear matter will be discussed in the next subsection.

E. Orbital angular momentum distribution of the deuteron in nuclear matter

The angular momentum structure of the deuteron wave function in nuclear matter is obtained from Eqs. (17), (28), and (30):

$$\begin{aligned} \langle \vec{k}, \sigma_p, \sigma_n | \phi(\vec{k}, \epsilon_M, M) \rangle \\ = \frac{N_M}{\epsilon_M - \epsilon_{K, L, L', \Lambda, \Lambda'}} \sum (L\Lambda, 1\sigma | 1M) Y_{L', \Lambda'}(\hat{k}) \\ \times \chi_{1\sigma}(\sigma_p, \sigma_n) v_L(k) \delta_{\Lambda', \Lambda} \\ \times Q_{L', L}^{\Lambda}(K, k, k_F), \end{aligned} \quad (37a)$$

where

$$\delta_{\Lambda', \Lambda} Q_{L', L}^{\Lambda}(K, k, k_F) = \int d\hat{k} Y_{L', \Lambda'}^*(\hat{k}) \theta_{k_F}(\vec{k}, \vec{k}) Y_{L\Lambda}(\hat{k}). \quad (37b)$$

The quantity $Q_{L', L}^{\Lambda}$ determines the way in which the orbital angular momentum structure of the deuteron is modified by the requirement that the neutron and proton both must have momenta outside the Fermi sea, and is related to the quantity θ_i introduced in Eq. (25) by

$$\begin{aligned} Q_{L', L}^{\Lambda} = \sum_i (L\Lambda, 10 | L'\Lambda) (L0, 10 | L'0) \\ \times \frac{\hat{L}^2}{2L'} \theta_i(K, k, k_F). \end{aligned} \quad (38)$$

Figures 5–7 are the results of calculations of

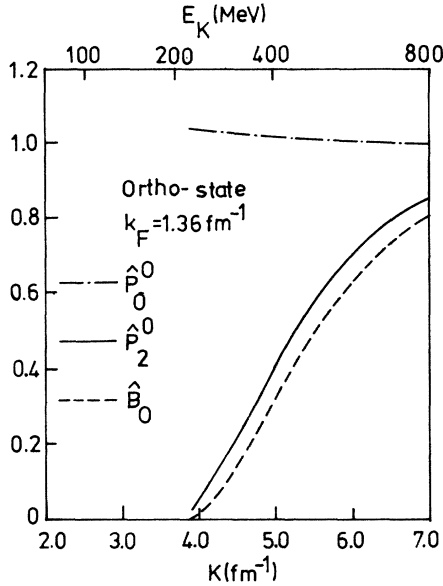


FIG. 5. Orbital angular momentum distribution in nuclear matter of Fermi momentum 1.36 fm^{-1} for the para state. The ratios are defined in Eqs. (41) and (42).

the probability distribution

$$P_L^M(K, k_F) \equiv \sum_{\Lambda, \sigma} \int_0^\infty dk k^2 |\langle k, L' \Lambda, 1\sigma | \phi(\vec{K}, \epsilon_M, M) \rangle|^2, \quad (39)$$

where, according to Eq. (37)

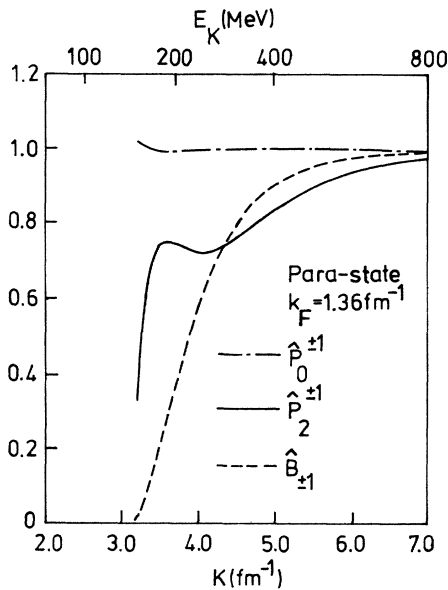


FIG. 6. As in Fig. 5, but for the ortho state.

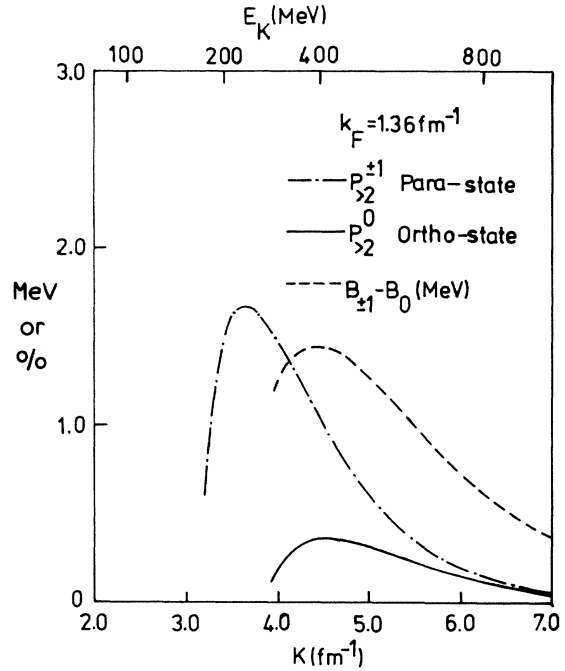


FIG. 7. High orbital angular momentum distribution in nuclear matter of Fermi momentum 1.36 fm^{-1} .

$$\langle k, L' \Lambda, 1\sigma | \phi(\vec{K}, \epsilon_M, M) \rangle = \frac{N_M}{\epsilon_M - \epsilon_k} \sum_L (L \Lambda, 1\sigma | 1M) Q_{L'L}^\Lambda \nu_L(k). \quad (40)$$

$P_L^M(K, k_F)$ is the probability of finding the orbital angular momentum L' in a deuteron with center-of-mass momentum K in nuclear matter of Fermi momentum k_F , and in either the ortho ($M=0$) or para state ($M=\pm 1$). Quantities shown with a circumflex in Figs. 5 and 6 refer to the ratios

$$\hat{P}_L^M(K, k_F) = \frac{P_L^M(K, k_F)}{P_L}, \quad (41a)$$

where $L=0$ and 2 , and P_L is the corresponding probability in free space as determined by the parameters given in Eq. (16), i.e., $P_2 = 4\%$.

The binding energy ratios

$$\hat{B}_M = B_M/B_f \quad (41b)$$

are also plotted in Figs. 5 and 6 for comparison purposes.

The most striking feature of the results shown in Figs. 5 and 6 is that the decrease in deuteron binding energy with decreasing center-of-mass momentum K is strongly correlated with a decrease in D -state probability. A comparison of Figs. 5 and 6 shows that the much slower decrease of the binding energy of the para state with K , noted in Sec. IID, is reflected in the much slower decrease

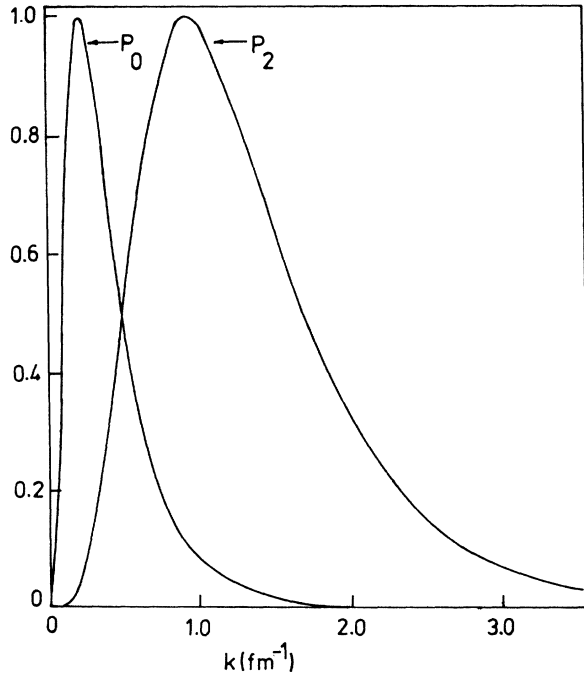


FIG. 8. Distribution of relative momenta in the S state (P_0) and the D state (P_2) corresponding to a D-state probability of 4%. P_0 and P_2 are normalized in such a way that their respective maxima are equal to one.

with K of the D-state probability in the para-state case.

These simple correlations break down when $|\frac{1}{2}K - k_F|$ is not large compared with the momentum spread in the free deuteron S-state wave function. An indication of the more complex situation for $K < 4 \text{ fm}^{-1}$ when $k_F = 1.36 \text{ fm}^{-1}$ is seen in Fig. 6. A full discussion is given in Ref. 15.

Figure 7 shows the behavior of the quantity

$$P_{>2}^M = \sum_{L=4}^{\infty} P_L^M(K, k_F). \quad (42)$$

It can be seen that the probability of orbital angular momentum values other than S and D remain very small for $K > 4 \text{ fm}^{-1}$, and this is reflected in the fact that the decrease in D-state probability mentioned above is mainly associated with an increase in the S-state probability. The qualitative features of these results can be understood as follows.

In the first place, for large center-of-mass momentum K , the role of the Pauli projection operator $Q_{\vec{K}}$ is to project out large relative momentum components k because it is only these components that can combine with $\frac{1}{2}\vec{K}$ to give a momentum less than k_F . The D-state component of the free-space deuteron wave function is peaked at much higher relative momenta than is the S-state

component (see Fig. 8). It is therefore natural that the effect of nuclear matter is to reduce the D-state probability, and thus reduce the effectiveness of the tensor force in producing binding.

Secondly, the large difference between the Pauli effects in the ortho and para states can be understood as the result of the absence of any component in the $M=0$ wave function with $L_x=2$. This can be seen in Eq. (37a) where the Clebsch-Gordan coefficient $(L\Lambda, 1\sigma | 1M)$ allows $\Lambda = \pm 2, \sigma = \mp 1$, if $M = \pm 1$, but if $M=0$, $\Lambda = -\sigma = \pm 1$, or 0 only. This simple consequence of angular momentum conservation is important because of the different dependence on k_F and K enjoyed by the quantity

$$Q_{22}^{\Lambda}(K, k, k_F) = \int d\hat{k} \theta_{\vec{k}_F}(\vec{K}, \vec{k}) |Y_{2\Lambda}(\hat{k})|^2 \quad (43)$$

for different values of Λ .

The influence of the Pauli principle on the D-state probability in the wave function Eq. (37a) appears through the deviation of Q_{22}^{Λ} from unity. For $\frac{1}{2}K > k_F$, which is the region of interest here, deviation from unity occurs only if k lies in the range

$$\frac{1}{2}K - k_F < k < \frac{1}{2}K + k_F, \quad (44)$$

and then

$$Q_{22}^{\Lambda}(K, k, k_F) = \int_0^{2\pi} d\phi \int_{\theta_b}^{\pi-\theta_b} \sin\theta d\theta |Y_{2\Lambda}(\theta, \phi)|^2, \quad (45)$$

where

$$\cos\theta_b = \frac{k^2 + \frac{1}{4}K^2 - k_F^2}{Kk} \equiv b \quad (46)$$

as defined in Eq. (27b).

It is readily shown that

$$Q_{22}^2 = \frac{1}{8}b(3b^4 - 10b^2 + 15), \quad (47a)$$

$$Q_{22}^1 = \frac{1}{2}b^3(5 - 3b^2), \quad (47b)$$

$$Q_{22}^0 = \frac{1}{4}b(9b^4 - 10b^2 + 5), \quad (47c)$$

and that as b deviates from 1, Q_{22}^2 drops off much more slowly from the value 1 than do Q_{22}^1 and Q_{22}^0 .

Hence the D-state part of a deuteron with $M=1$ contains a large proportion (60% in free space) of a component which is relatively unaffected by the Fermi sea if $\frac{1}{2}K \gg k_F$. The ortho state has a D-state part which consists entirely of components with $\Lambda=0$ and ± 1 and which are affected strongly by the Pauli projection. The much stronger effect of the Fermi sea on the binding energy of the ortho state than on the para state is therefore understandable.

The effects of changes of P_D on the binding energies and binding energy differences in the region $\frac{1}{2}K \gg k_F$ in Figs. 1-4 also now become clearer.

TABLE I. Calculated parameters for the Yamaguchi potential and the corresponding triplet effective range.

<i>D</i> -state probability (%)	Effective range r_0 (fm)	β (fm ⁻¹)	γ (fm ⁻¹)	λ (fm ⁻³)	t
1	1.704	1.415	0.6773	0.382 0	0.1124
2	1.705	1.388	1.077	0.342 2	0.4701
3	1.704	1.361	1.337	0.297 9	0.9946
4	1.702	1.335	1.537	0.254 0	1.663
5	1.701	1.309	1.701	0.213 8	2.467
6	1.699	1.284	1.841	0.178 6	3.401
7	1.697	1.260	1.963	0.148 7	4.463
8	1.695	1.237	2.072	0.123 8	5.652
9	1.693	1.214	2.170	0.103 2	6.971
10	1.691	1.191	2.259	0.086 22	8.419

For the parameter changes discussed in the Appendix an increase in P_D is associated with a decrease in the range of the V_{np} tensor force, i.e., an increase in the parameter γ in Table I. Hence the *D*-state wave function extends to higher momentum, and is enhanced in a region of momentum where the Pauli projection operator differs from unity. The net effect is to project out more of the *D*-state wave function in a range of momentum where the tensor force is large and hence to decrease the latter's binding effect even further. This is the effect of increasing P_D shown in Figs. 1 and 3. The effect of increasing P_D shown in Figs. 2 and 4 reflects the fact, discussed in the last paragraph, that the Pauli projection has a relatively small effect on those angular momentum components which dominate the para states but are absent from the ortho state.

A simple physical picture which correctly accounts for many of the features discussed above is described in the next subsection.

F. A simple picture

The basic mechanism whereby the influence of the nuclear medium causes the binding energy of the deuteron to depend on $\vec{J} \cdot \vec{K}$ can be understood in terms of a model in which the intrinsic spins of the nucleons in the deuteron are ignored and the "spin" of the deuteron is accounted for entirely in terms of orbital angular momentum, $L=1$. For this fictitious deuteron¹⁸ there is a very strong correlation between the plane of the orbit of the neutron and proton about their center of mass and the value of L_z the projection of the deuteron "spin" along \vec{K} .

If the proton in the deuteron has momentum \vec{k} relative to the deuteron center of mass, then the presence of the nuclear medium means that \vec{k} must satisfy

$$|\frac{1}{2}\vec{K} + \vec{k}| > k_F, \quad (48a)$$

and

$$|\frac{1}{2}\vec{K} - \vec{k}| > k_F. \quad (48b)$$

For a deuteron with $L_z = \pm 1$, when semiclassically the plane of the *n-p* orbit in which the rotating vector \vec{k} lies is always perpendicular to \vec{K} , the conditions (48a) and (48b) reduce to

$$(\frac{1}{4}K^2 + k^2)^{1/2} > k_F, \quad (49)$$

because \vec{k} and \vec{K} are perpendicular in this case.

However, if $L_z = 0$, then for part of the time \vec{k} must have a component along \vec{K} and the conditions (48a) and (48b) become

$$(\frac{1}{4}K^2 + k^2 + \vec{k} \cdot \vec{K})^{1/2} > k_F, \quad (50a)$$

$$(\frac{1}{4}K^2 + k^2 - \vec{k} \cdot \vec{K})^{1/2} > k_F. \quad (50b)$$

For a given K , if the magnitude of \vec{k} is such that condition (49) is just satisfied it is clear that conditions (50) will be violated for some orientation of \vec{k} . Hence if the range of possible values of k^2 has an upper bound, as it does effectively in the deuteron, the condition (49) is more easily satisfied than conditions (50), i.e., it is harder to satisfy the Pauli principle in the case $L_z = 0$ than in the case $L_z = \pm 1$. This simple model therefore predicts that the state with $L_z = 0$ is more strongly affected by the presence of the nuclear medium than states with $L_z = \pm 1$.

The crucial property of the fictitious deuteron used in this argument is the coupling between the plane of the orbit of the neutron and proton about their center of mass and the projection of the deuteron "spin." A coupling of this type is contained in the real deuteron through its *D*-state component. The quantum analog of the discussion of conditions (49) and (50) is the discussion in the last subsection of the properties of the quantities Q_{22}^A

as a function of Λ and the way in which values of Λ are linked with values of M in the deuteron D -state component.

III. SPIN DEPENDENCE OF THE DEUTERON OPTICAL POTENTIAL

A. Nuclear matter

The results of the last section show that the dispersion law for a bound deuteron with $J_z = M$, total energy E , and center-of-mass momentum \vec{K} , in nuclear matter of Fermi momentum k_F , is

$$E = \epsilon_M(K, k_F) + \frac{\hbar^2 K^2}{4m} + U_p^{(0)} + U_n^{(0)}, \quad (51)$$

where the notation is that of Eqs. (7).

The quantity

$$V_M(K, k_F) = \epsilon_M - \epsilon_f + U_p^{(0)} + U_n^{(0)}, \quad (52)$$

where ϵ_f ($= -B_f$) is the value of ϵ_M in free space, can be interpreted as an effective potential for a deuteron propagating in nuclear matter, i.e., the deuteron optical potential.

The contribution to V_M from the binding energy modification can be written

$$\epsilon_M - \epsilon_f = \Delta\epsilon_c - \Delta\epsilon(M^2 - \frac{2}{3}), \quad (53)$$

where

$$\Delta\epsilon_c(K, k_F) = \frac{2}{3}\epsilon_1 + \frac{1}{3}\epsilon_0 - \epsilon_f, \quad (54a)$$

$$\Delta\epsilon(K, k_F) = \epsilon_0 - \epsilon_1 = B_1 - B_0, \quad (54b)$$

and $\Delta\epsilon$ is the quantity plotted in Figs. 2 and 4.

The term $\Delta\epsilon_c$ in Eq. (53) is a Pauli correction to the spin-independent part of the deuteron optical potential and is related to the corrections estimated in Refs. 1-6.

Recalling the definition of M , the spin-dependent term in Eq. (53) can be written

$$- \frac{\Delta\epsilon}{K^2} [(\vec{S} \cdot \vec{K})^2 - \frac{2}{3}K^2], \quad (55)$$

where \vec{S} is the spin-1 operator, i.e., the operator denoted by \vec{J} for clarity hitherto.

The spin-dependent potential (55) has the form of a second rank tensor potential of the T_p type, in the original classification of Satchler,⁷ where

$$T_p = (\vec{S} \cdot \vec{K})^2 - \frac{2}{3}K^2. \quad (56)$$

There are another two types of spin-dependent second rank tensor forces which do not violate general symmetry requirements, and which in principle could be present in the deuteron optical potential in addition to the usual $\vec{L} \cdot \vec{S}$ potential. According to Satchler⁷ these are

$$U_1(R)T_R, \quad (57a)$$

$$U_2(R)T_L, \quad (57b)$$

where

$$T_R = \left(\frac{\vec{S} \cdot \vec{R}}{R} \right)^2 - \frac{2}{3}, \quad (58a)$$

$$T_L = (\vec{L} \cdot \vec{S})^2 + \frac{1}{2}\vec{L} \cdot \vec{S} - \frac{2}{3}\vec{L}^2, \quad (58b)$$

and where U_1 and U_2 are arbitrary radial functions.

Terms of the T_R and T_L type cannot occur in the dispersion law for a deuteron propagating in nuclear matter of constant density.

B. Finite size target nucleus

It was shown in the previous subsection that the combined effect of the Pauli principle and the tensor force component in V_{np} is to generate a tensor force of the T_p type in the nuclear matter case. The calculation of the T_p force in the deuteron-nucleus optical potential requires an approximate solution of Eq. (1) in the case that U_p , U_n , and Q have the forms appropriate to a finite target nucleus. The calculations presented in the next subsection are based on the following approximations and assumptions.

(i) We assume that at each center-of-mass coordinate \vec{R} that the center-of-mass motion is associated with a definite local momentum $\vec{K}(\vec{R})$. This is the approach used, for example in Refs. 5 and 6, and in effect replaces the operator QV_{np} by one which is local in the variable \vec{R} (but not necessarily in the variable \vec{r}).

(ii) All breakup effects due to the potentials U_p and U_n are ignored, and U_p and U_n are replaced in Eq. (1) by the Watanabe¹⁷ deuteron optical potential

$$\langle \vec{R}', M' | V_0 | \vec{R}, M \rangle = \langle \vec{R}', \phi_M | U_p + U_n | \vec{R}, \phi_M \rangle, \quad (59)$$

where $\phi_M(\vec{r})$ is the free-space deuteron wave function. The notation in Eq. (59) allows for the fact that the optical potentials U_p and U_n may be non-local. Corrections to this approximation, in the absence of Pauli effects, have received considerable attention^{3,18,19} and definitely cannot be ignored in general.²⁰

(iii) At each point R the relative motion of the neutron and proton of the incident deuteron is assumed to be a bound state solution of the equation

$$[\epsilon(R) - t_r - Q_R(R)V_{np}]\phi(\vec{r}, \vec{R}) = 0. \quad (60)$$

If τ_R is the time taken by the center of mass to travel a distance ΔR , for which the perturbation $(Q_R - 1)V_{np}$ changes appreciably and τ_r is the time which characterizes the components of the n - p relative motion that are mainly affected by the perturbation $(Q_R - 1)V_{np}$ in Eq. (60), a qualitative estimate for the validity of the adiabatic assumption (iii) can be set by requiring that $\tau_R \gg \tau_r$. The ef-

fect of the Pauli principle when $\frac{1}{2}K > k_F$ is to project out relative momenta K satisfying

$$k > \frac{1}{2}K - k_F \quad (61)$$

and for these components

$$\frac{\tau_p}{\tau_R} < \frac{2}{\Delta R} \frac{K}{(K - 2k_F)^2} \cdot \quad (62)$$

If R is taken to be the surface thickness of the target, a discussion based on estimate (62) shows that approximation (iii) is expected to have some validity in the nuclear surface for incident deuteron energies in excess of 100 MeV, and to become rapidly more valid as the energy increases. Detailed quantitative considerations concerning the validity of approximation (ii) and (iii) will be given elsewhere.²¹

(iv) The projection operator $Q_{\vec{K}}(\vec{R})$ is assumed to be given by Eq. (8), where $k_F(R)$ is determined by the target density $\rho(R)$ at R through the relation

$$k_F(R) = \left\{ \frac{1}{2} [3\pi^2 \rho(R)] \right\}^{1/3}. \quad (63)$$

Approximation (iv) is closely related to the approximate form for the one-body density matrix for finite nuclei which has been found to have a useful range of validity by Negele and Vautherin.²² In the present context it is important to note that it is the nuclear density averaged over a distance characterizing the range of V_{np} , and not over the size of the deuteron, which determines the size of the Pauli effect. This is reflected by the structure of Eqs. (1) and (60). Note also that the calculations of Sec. II show that the splitting $\Delta\epsilon$ is very sensitive to the properties of V_{np} for high values of k . Thus $\Delta\epsilon$ is associated with rather close collisions of the neutron and proton, and an estimate based on the target density at their center of mass should not be a bad approximation.

C. Results for finite nuclei

The result of the approximations discussed in Sec. II B is to replace the dispersion relation (51) for an incident deuteron kinetic energy E_d ($\equiv E + B_f$) by

$$E_d = \frac{\hbar^2 K^2}{4M} + V_0(R, K) + \Delta\epsilon_c(R, K) - \Delta\epsilon(R, K)(M^2 - \frac{2}{3}), \quad (64)$$

where V_0 , $\Delta\epsilon_c$, and $\Delta\epsilon$ are defined in Eqs. (59), (54a), and (54b), respectively, and $M = \pm 1, 0$.

The binding energy corrections $\Delta\epsilon_c$ and $\Delta\epsilon$ in Eq. (64) acquire an R dependence because of their dependence on the local Fermi momentum $k_F(R)$. The latter has been calculated from Eq. (63) with ρ obtained from the Fermi charge distributions²³ given in Table 3 of Ref. 24.

For a given incident energy E_d and spin projection M , Eq. (64) is to be solved for K as a function of R . Denoting this solution by $K_M(R)$, the spin-dependent Pauli correction at R is

$$-\Delta\epsilon[R, K_M(R)](M^2 - \frac{2}{3}). \quad (65)$$

Because of the smallness of $\Delta\epsilon_c$ and $\Delta\epsilon$ compared with V_0 and the known properties of the latter, this procedure can be simplified considerably, and to sufficient accuracy $K(R)$ can be taken to be the solution of

$$E_d = \frac{\hbar^2 K^2}{4M} + V_n(R) + V_p(R) + V_{\text{coul}}(R), \quad (66)$$

where V_n and V_p are neutron and proton optical potentials evaluated^{9,10} at $\frac{1}{2}E_d$ and V_{coul} is the Coulomb field of the target. The spin-orbit and imaginary parts of V_n and V_p are neglected, as is the effect of averaging over the deuteron internal wave function in Eq. (59). In considering these approximations it should be borne in mind that for the incident energies of main interest here $K(R)$ is a much more slowly varying function of R than is $k_F(R)$. Hence, errors in $K(R)$ do not produce large errors in the R dependence of the ratio $K/2k_F$, which is the key parameter determining the magnitude of the Pauli effects.

The values of V_p and V_n were calculated using the parameters given in Ref. 25, Eq. (13). The potential V_{coul} was taken to be that due to a uniformly charged sphere of charge radius R_c .²⁶ Once again the fact that these potentials do not give accurate fits to nucleon scattering at the higher end of the energy range considered here is of little importance because for high energy $K(R)$ is dominated by E_d .

Results for a ^{92}Zr target calculated in the manner outlined above are shown in Figs. 9–14 for several incident deuteron energies and free-space D -state probabilities (determined as discussed in Sec. II C). Figures 9–11 display the ratios B_M/B_f as a function of R , and Figs 12–14 display the splitting $\Delta\epsilon(R)$ defined in Eq. (54b). Results obtained for other targets display the same qualitative features as the ones shown here.

For incident deuteron energies in the neighborhood of 50 MeV (Fig. 9) the binding energy of the ortho state reduces rapidly to zero just inside the nuclear surface. The binding energy of the para state is also reduced as the deuteron penetrates the nuclear surface but remains finite and constant in the nuclear interior. The binding energy difference $\Delta\epsilon$ (Fig. 12) has been calculated only when both the para-state and ortho-state configurations are bound. At these energies $\Delta\epsilon$ exhibits a peak at the nuclear surface, just before B_0 vanishes.

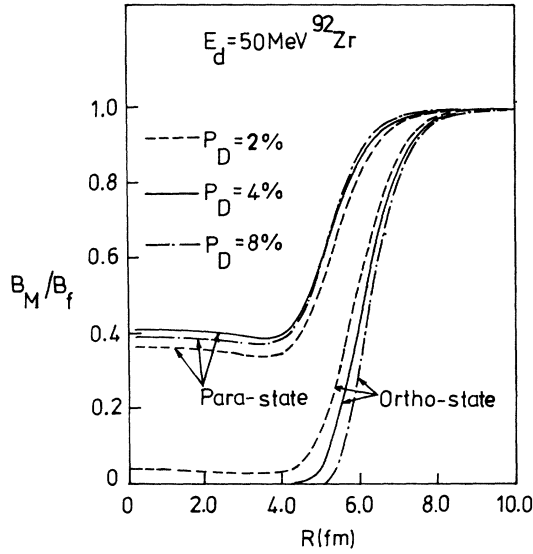


FIG. 9. The ratios of the binding energy of the deuteron in a finite nucleus to the free-space binding energy, for the ortho state and para state, for various D -state probabilities at $E_d = 50$ MeV.

At higher incident energies (Figs. 10 and 11) both the para- and ortho-state configurations are bound throughout the target nucleus. The binding energy reduction is much greater for the ortho state than for the para state at a particular value of R . The energy difference $\Delta\epsilon$ (Figs. 13 and 14) is almost constant in the nuclear interior and falls rapidly to zero outside the nuclear surface.

As a function of energy the maximum value of

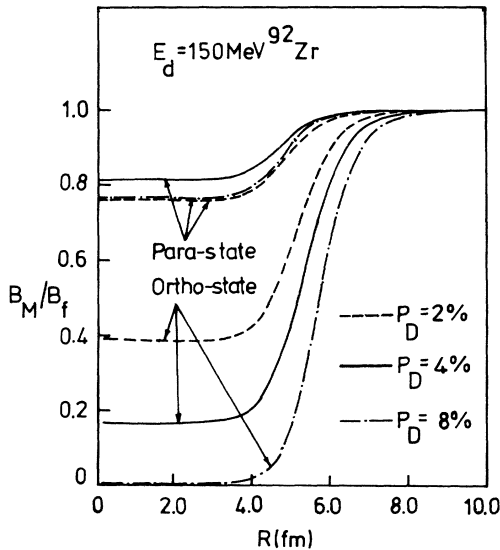


FIG. 10. As in Fig. 9 but for $E_d = 150$ MeV.

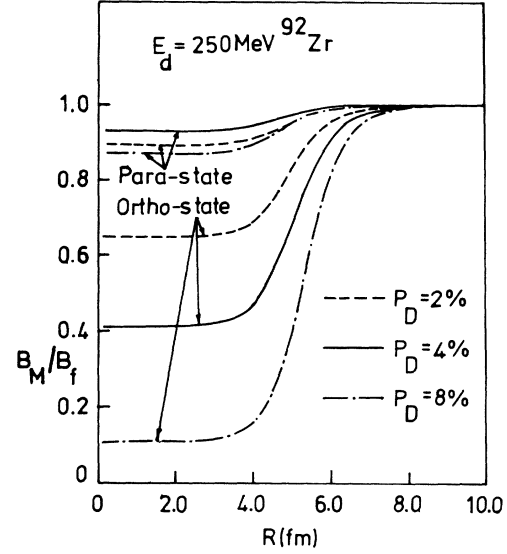


FIG. 11. As in Fig. 9 but for $E_d = 250$ MeV.

the energy difference $\Delta\epsilon(R)$ has a maximum at about 180 MeV, the precise energy depending on P_D and the target. This behavior reflects the fact that for zero local momentum $K(R)$ there can be no splitting of states with different M because no direction is picked out. At high energies when $K(R) \gg k_F(R)$ for all R , the Pauli principle has no effect because for these values of K there is a negligible probability of finding either nucleon of the deuteron with a momentum less than k_F . In this limit the Pauli correction is small and $Q \sim 1$. For any deuteron wave function of the form

$$\Phi_M(\vec{k}) = [u_S(k) + S_{12}u_D(k)] \chi_1^M \quad (67)$$

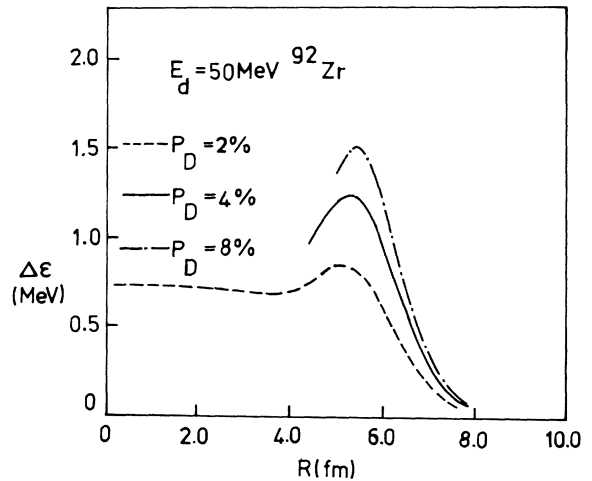
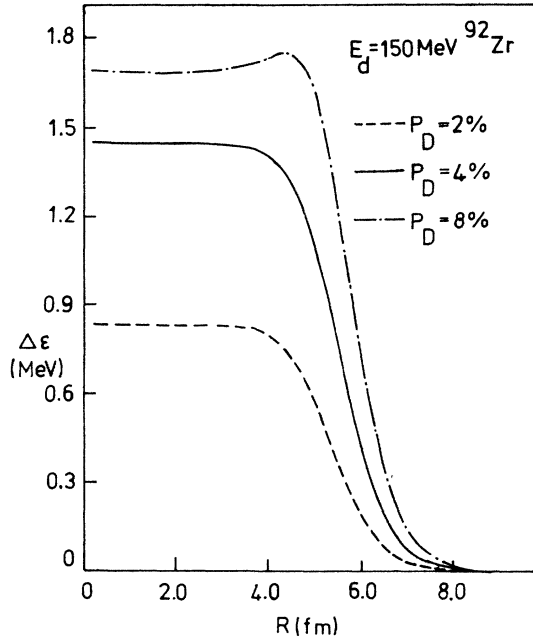


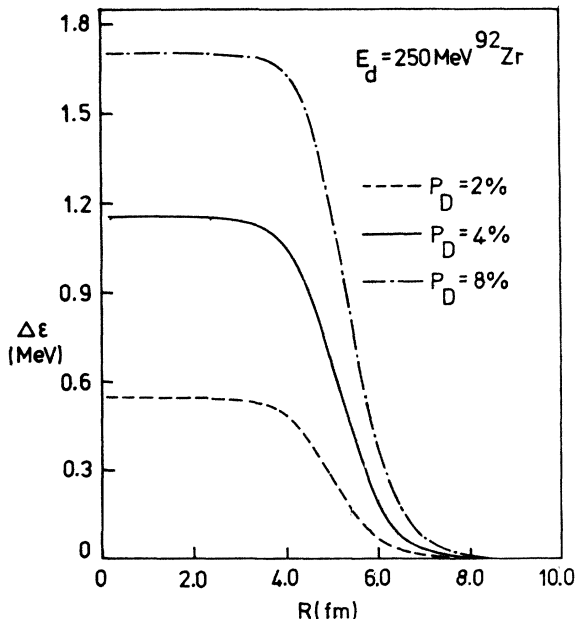
FIG. 12. Binding energy difference between the para state and ortho state in a finite nucleus for $E_d = 50$ MeV.

FIG. 13. As in Fig. 12 but for $E_d = 150$ MeV.

$\Delta\epsilon$ can be estimated from the perturbation theory result

$$\Delta\epsilon \approx \langle \Phi_1 | Q V_{np} | \Phi_1 \rangle - \langle \Phi_0 | Q V_{np} | \Phi_0 \rangle \quad (68)$$

which yields

FIG. 14. As in Fig. 12 but for $E_d = 250$ MeV.

$$\Delta\epsilon(R, K) \approx 48\pi^3 \rho(R) (E_d + B_f) u_D(\frac{1}{2}K) \times [u_D(\frac{1}{2}K) - u_s(\frac{1}{2}K)]. \quad (69)$$

An idea of the validity of this formula can be obtained from a comparison of the prediction of Eq. (69) with the results for the Yamaguchi potential described in previous sections. The two methods agree to within 15% for all nuclear densities for $E_d \geq 300$ MeV and for nuclear regions beyond the half-density radius for lower energies. Equation (69) clearly exhibits the dependence of $\Delta\epsilon$ on the momentum distribution in the deuteron. It can be used to estimate $\Delta\epsilon$ for any assumed V_{np} interaction. Calculations along these lines are in progress.

The magnitude of $\Delta\epsilon$ increases significantly as the free-space D -state probability increases. This is the analog of the phenomenon discussed at the end of Sec. II E for nuclear matter, and can also be deduced from the approximate result given in Eq. (69).

The detail shape of $\Delta\epsilon(R)$ can be very well fitted to the form

$$\Delta\epsilon(R) = V_1 \{1 + \exp[(R - c_1)/a_1]\}^{-1} + V_2 \exp[(R - c_2)/a_2] \times \{1 + \exp[(R - c_2)/a_2]\}^{-2}, \quad (70)$$

where the parameters V_1 etc. vary with energy and target.

The second term in Eq. (70) is important for $E_d \leq 180$ MeV, where it contributes to a surface peak in $\Delta E(R)$.

D. T_p potential

As discussed in Sec. III A the splitting $\Delta\epsilon$ gives information about the strength of a potential of the T_p type in the deuteron optical potential [see Eqs. (55) and (56)].

It is interesting to compare the values of $\Delta\epsilon$ with the strength of the T_R potential predicted by the Watanabe model. According to Keaton and Armstrong²⁷ the latter model predicts a peak value in the nuclear surface of about 2 MeV for a medium mass nucleus (^{60}Ni) at $E_d = 15$ MeV. At $E_d = 180$ MeV this predicted value will be reduced to about 1.0 MeV if it is assumed that the energy dependence of the nucleon optical potential is given by $dU_n/dE_p = 0.3$. In the neighborhood of $E_d = 180$ MeV the T_p potential predicted by the calculation of the last section has a maximum strength, the value at maximum varying from 0.8 to 1.7 MeV depending on the properties of the n - p interaction at short distances.

These considerations suggest that the Pauli mechanism makes an important contribution to

the spin dependence of the deuteron-nucleus interaction at energies in the 100–300 MeV range.

At lower energies the treatment of the Pauli effects used here is expected to break down. Nevertheless the basic mechanism which produces the T_p force is still operative at low energies, although an accurate estimate of its strength becomes more difficult. Calculations²¹ based on the present method and on the alternative approach of Austern²⁸ give a T_p force of magnitude similar to the T_R force predicted by the Watanabe model, although of considerably smaller diffuseness. From a phenomenological point of view Goddard has shown²⁹ that at low energies it can be difficult to differentiate the effects of a T_R and T_p force on observables.

IV. CONCLUSIONS

A definite physical mechanism has been proposed which generates a spin-dependent interaction of novel type in the deuteron-nucleus interaction. Approximate calculations indicate that this force should play a very important role in the spin dependence of deuteron scattering from spin-zero nuclei at energies below approximately 400 MeV.

A key feature of this spin-dependence is its second rank tensor character. As a result³⁰ the observables T_{20} , T_{21} , and T_{22} and certain combinations of polarization transfer coefficients³¹ are expected to be most strongly effected by the presence of this force.

It was shown in Sec. II E that the strong spin-dependence discussed here arises because the Pauli principle strongly inhibits the ability of the tensor force in V_{np} to contribute to the binding of a deuteron in nuclear matter. It is interesting that a similar mechanism is believed to play an important role in the understanding of the saturation properties of nuclear forces.³² In nuclear matter calculations one important reason why a minimum occurs in the binding energy-density curve near the observed density of nuclear matter is because the binding energy contribution from two nucleons in a 3S_1 state below the top of the Fermi sea is strongly influenced by the suppression of tensor force effects by the requirements of the Pauli principle.³² In the nuclear matter ground state all directions of the center-of-mass momentum of a pair of nucleons are equally probable and are averaged over in the calculation of the energy of nuclear matter. Hence, the splitting of states with different values of $\vec{J} \cdot \vec{K}$ by the Pauli mechanism is of secondary importance. On the other hand, in the case of deuteron scattering the incident and scattered beam momenta pick out directions for \vec{K} of special significance, and the splitting effects become ob-

servable through their influence on the polarization of the scattered deuterons. In principle a study of the strength of the T_p force provides information on the effective interaction in nuclear matter for a range of energies and densities.

It was shown in Sec. III C that the predicted strength of the T_p force is very sensitive to the properties of the n - p interaction at short distances. These results were obtained using the rather crude Yamaguchi model of the n - p interaction. However, it was shown in Sec. II C that the Yamaguchi potential is sufficiently flexible that its low energy properties can be kept fixed while at the same time altering its high energy properties. The qualitative point made in Sec. III C is expected, therefore, to survive a more complete calculation.

An important feature of deuteron wave functions generated by forces more realistic than the Yamaguchi potential, and which therefore contain a hard core, is that the momentum space S -state wave function has a zero in the neighborhood of 2 fm^{-1} where the D -state wave function is very large.³³ In the same momentum range the S and D components of the Yamaguchi wave function have a very similar magnitude. Hence for high incident deuteron energies the effect of the Pauli principle in projecting out high momentum components, as discussed in Sec. II E, will have a much bigger effect on the D -state wave function, relative to the effect on the S -state wave function, in the hard core case than in the Yamaguchi case. On these grounds alone, therefore, it is expected [see, e.g., Eq. (69)] that a more realistic V_{np} will generate an even larger T_p force than that generated by the Yamaguchi potential and reported here.

Another aspect of the Pauli mechanism investigated in Sec. II E is that, in addition to predicting a T_p force it also has implications for the T_R force. According to the Watanabe model the latter depends on the D -state component of the deuteron in a crucial manner.^{27,34-36} It was shown in Sec. II E that the Pauli principle changes the deuteron D -state probability from its free-space value. For high enough energy the effect is always to decrease the D -state probability at any density, but at lower energy the effects are more complicated. In any case, it is clear that modifications are expected of the predictions of the Watanabe model with a free-space deuteron wave function, and may produce interesting effects on tensor analyzing powers in elastic deuteron scattering at low energies.^{27,29,36}

ACKNOWLEDGMENTS

This work received considerable stimulus from discussions of the role of the Pauli principle in

deuteron scattering between one of the authors (R.C.J.) and J. J. Griffin and B. L. Gambhir while R.C.J. was on leave at the University of Maryland during September 1974. The authors are grateful to R. P. Goddard, W. S. Pong, and G. Rawitscher for information about their work prior to publication and for stimulating and useful discussions. The computing assistance of J. Hilton and the University of Surrey Computing Unit was indispensable. Many of the ideas involved in this work were clarified while R.C.J. was on leave during 1976 at the University of Maryland (supported in part by the U. S. Energy Research Development Association) and at the University of Wisconsin where he was supported by a grant from the General Electric Foundation. The work at Surrey by A.I. was supported by the Science Research Council and a University Studentship.

APPENDIX

The Yamaguchi potential contains four parameters. They are β and γ , which are associated with the range of the central and tensor interaction, the overall strength of the n - p interaction

λ , and the relative strength of the tensor interaction t . For given D -state probability P_D , the properties of the deuteron and the experimental value for the triplet scattering length a permit only one set of physically meaningful parameters for the Yamaguchi potential.¹² This set of parameters is obtained as follows.^{12,15}

The quantity Δ is fixed from the experimental value of the deuteron binding energy. Equations (25) and (29) in Ref. 12 for P_D and a yield the following third order equation in γ and β :

$$\frac{2(1-P_D)}{P_D} \left(\frac{\Delta+\beta}{\beta} \right)^3 \left[\frac{1}{a\Delta} - \frac{\beta(\Delta+2\beta)}{2(\Delta+\beta)^2} \right] = \frac{\Delta+\gamma}{\gamma(5\Delta+\gamma)} \left[2\Delta + \frac{(\Delta+\gamma)^2}{\gamma} \right]. \quad (A1)$$

For assumed values of β and P_D this equation has only one real solution for γ . The overall strength of the interaction λ and the relative strength of the tensor force t may then be determined from Eqs. (23) and (25) of Ref. 12. With these values for Δ , β , γ , λ , and t , the deuteron quadrupole moment Q is determined from the expression

$$Q = \frac{\sqrt{2}\pi^2 N^2 t}{10(\Delta+\beta)^4} \left[\frac{\Delta^{-1}}{(\beta+\gamma)^2(\Delta+\gamma)^5} \{ \Delta\beta^2(5\Delta^2+4\Delta\beta+\beta^2) + \beta\gamma(10\Delta^3+33\Delta^2+22\Delta\beta^2+5\beta^3) \right. \\ \left. + \gamma^2(5\Delta^3+22\Delta^2+33\Delta\beta^2+10\beta^3) + \gamma^3(\Delta^2+4\Delta\beta+5\beta^2) \} \right. \\ \left. + \frac{2}{(\beta+\gamma)^3(\Delta+\gamma)^4} \{ \Delta(\beta+\gamma)^3 + 4(\Delta^2+\beta\gamma)(\beta^2+3\beta\gamma+\gamma^2) + 16\Delta\beta\gamma(\beta+\gamma) \} \right. \\ \left. + \frac{2}{(\beta+\gamma)^4(\Delta+\gamma)^3} \{ \beta(\Delta+\gamma)^3 + 4(\beta^2+\Delta\gamma)(\Delta^2+3\Delta\gamma+\gamma^2) + 16\Delta\beta\gamma(\Delta+\gamma) \} \right] \\ - \frac{\pi^2 N^2 t^2 (7\Delta^3+49\Delta^2\gamma+91\Delta\gamma^2+33\gamma^3)}{160\gamma^3(\Delta+\gamma)^7}. \quad (A2)$$

This expression is reproduced here because the corresponding expression in Ref. 12, Eq. (26), is incorrect.

For a fixed value for P_D , the above procedure yields two sets of parameters corresponding to a given value of Q . One of these two sets, however, corresponds to an unphysically long range for the tensor interaction (~ 10 fm) and it is therefore rejected.

The procedure outlined above yields only one set of parameters for the Yamaguchi potential for a given P_D . The triplet effective range corresponding to these sets varies little with P_D and has a reasonable value.

The calculated parameters for the Yamaguchi potential and the corresponding triplet effective

range are shown in Table I for a number of D -state probabilities. We have used the following values^{37,38} for Δ , a , and Q :

$$\Delta = 0.2316 \text{ fm}^{-1} \quad (B_f = 2.226 \text{ MeV}),$$

$$a = 5.378 \text{ fm},$$

$$Q = 0.2739 \text{ fm}^2.$$

The value of Q quoted above³⁸ has been recently reestimated³⁹ at $Q = 0.2860 \pm 0.0015 \text{ fm}^2$. A positive contribution to Q , due to exchange current effects, has been recently estimated⁴⁰ to be of order 0.01 fm^2 . The classical part of Q , relevant to the present discussion, is therefore expected to be close to the value employed.

- ¹G. Baumgartner, Z. Phys. 204, 17 (1967).
- ²P. J. R. Soper, Ph.D. thesis, University of Surrey, England, 1969 (unpublished).
- ³R. C. Johnson and P. J. R. Soper, Phys. Rev. C 1, 976 (1970).
- ⁴B. L. Gambhir and J. J. Griffin, Phys. Rev. C 7, 590 (1973).
- ⁵W. S. Pong and N. Austern, Ann. Phys. (N.Y.) 93, 369 (1975).
- ⁶D. G. Perkin, A. M. Kobos, and J. R. Rook, Nucl. Phys. A245, 343 (1975).
- ⁷G. R. Satchler, Nucl. Phys. 21, 116 (1960).
- ⁸A. A. Ioannides and R. C. Johnson, Phys. Lett. 61B, 4 (1976).
- ⁹R. C. Johnson and P. J. R. Soper, Nucl. Phys. A182, 619 (1972).
- ¹⁰P. D. Kunz, Phys. Lett. 35B, 16 (1971).
- ¹¹Y. Yamaguchi, Phys. Rev. 95, 1628 (1954).
- ¹²Y. Yamaguchi and Y. Yamaguchi, Phys. Rev. 95, 1635 (1954).
- ¹³D. M. Brink and G. R. Satchler, *Angular Momentum* (Clarendon, Oxford, 1968), 2nd ed., Chap. V, Sec. 5.3.
- ¹⁴Brink and Satchler, see Ref. 13, Chap. III, Tables 3 and 4.
- ¹⁵A. A. Ioannides, Ph.D. thesis, University of Surrey, England, 1976 (unpublished).
- ¹⁶The fact that this deuteron has opposite parity to that of the usual deuteron has no relevance to the present discussion.
- ¹⁷S. Watanabe, Nucl. Phys. 8, 484 (1958).
- ¹⁸G. H. Rawitscher, Phys. Rev. C 9, 2210 (1974).
- ¹⁹J. P. Farrel, Jr., C. M. Vincent, and N. Austern, Ann. Phys. (N.Y.) 96, 333 (1975).
- ²⁰For a review of three-body effects in reactions involving deuterons, see E. F. Redish, Topics in Current Physics 2, 181 (1976).
- ²¹A. Ioannides, W. S. Pong, and R. C. Johnson (unpublished).
- ²²J. W. Negele and D. Vautherin, Phys. Rev. C 5, 1472 (1972).
- ²³The electromagnetic size of the proton has not been unfolded from ρ . Errors due to this neglect are negligible for the purposes of the present work.
- ²⁴R. Engfer et al., At. Data Nucl. Data Tables 14, 509 (1974).
- ²⁵F. Becchetti and G. W. Greenlees, Phys. Rev. 182, 1190 (1969).
- ²⁶R. C. Barrett and D. F. Jackson, *Nuclear Sizes and Structure* (Oxford U. P., London, 1977).
- ²⁷P. W. Keaton, Jr. and D. D. Armstrong, Phys. Rev. C 8, 1692 (1973).
- ²⁸N. Austern, Phys. Lett. 61B, 7 (1976).
- ²⁹R. P. Goddard, Nucl. Phys. A291, 13 (1977).
- ³⁰D. J. Hooton and R. C. Johnson, Nucl. Phys. A175, 583 (1971).
- ³¹M. H. Lopes and F. D. Santos, Nucl. Phys. A283, 77 (1977).
- ³²H. A. Bethe, Annu. Rev. Nucl. Sci. 21, 95 (1971).
- ³³See, e.g., F. D. Santos, Ph.D. thesis, University of London, England, 1967 (unpublished); E. Rost and J. R. Shepard, Phys. Lett. 59B, 413 (1975).
- ³⁴L. D. Knutson and W. Haeberli, Phys. Lett. 30, 986 (1973).
- ³⁵L. D. Knutson and W. Haeberli, Phys. Rev. C 12, 1469 (1975).
- ³⁶O. Karban, A. K. Basak, J. A. R. Griffith, S. Roman, and G. Tungate, Nucl. Phys. A266, 413 (1976).
- ³⁷E. Lomon and R. Wilson, Phys. Rev. C 9, 1329 (1974) and references therein.
- ³⁸H. Narumi and T. Watanabe, Prog. Theor. Phys. 35, 1154 (1966); 36, 1313 (1966).
- ³⁹R. V. Reid, Jr., and M. L. Vaida, Phys. Rev. Lett. 29, 494 (1972); 34, 1064 (1975).
- ⁴⁰A. D. Jackson, A. Lande, and D. O. Riska, Phys. Lett. 55B, 23 (1975).